Check for updates

How to cite: *Angew. Chem. Int. Ed.* **2021**, *60*, 15613–15621
International Edition: doi.org/10.1002/anie.202102153
German Edition: doi.org/10.1002/ange.202102153

Drug Discovery **Hot Paper**

Antiprotozoal Structure–Activity Relationships of Synthetic Leucinostatin Derivatives and Elucidation of their Mode of Action

Michael Brand, Lei Wang, Stefano Agnello, Silvia Gazzola, Flavio M. Gall, Luka Raguž, Marcel Kaiser, Remo S. Schmidt, Amélie Ritschl, Jennifer Jelk, Andrew Hemphill, Pascal Mäser, Peter Bütikofer, Michael Adams, and Rainer Riedl**

Abstract: *Leucinostatin A is one of the most potent antiprotozoal compounds ever described, but little was known on structure–activity relationships (SAR). We used Trypanosoma brucei as a protozoal model organism to test synthetically modified derivatives, resulting in simplified but equally active compounds* ***2*** *(ZHAWOC6025) and* ***4*** *(ZHAWOC6027), which were subsequently modified in all regions of the molecule to gain an in-depth SAR understanding. The antiprotozoal SAR matched SAR in phospholipid liposomes, where membrane integrity, leaking, and dynamics were studied. The mode of action is discussed based on a structure–activity analysis of derivatives in efficacy, ultrastructural studies in T. brucei, and artificial membrane models, mimicking membrane stability and membrane potential. The main site of antiprotozoal action of natural and synthetic leucinostatins lies in the destabilization of the inner mitochondrial membrane, as demonstrated by ultrastructural analysis, electron microscopy and mitochondrial staining. Long-time sublethal exposure of T. brucei (200 passages) and siRNA screening of 12′000 mutants showed no signs of resistance development to the synthetic derivatives.*

Introduction

Leucinostatins, antimicrobial peptides (AMPs) from the biocontrol agent *Purpureocillium lilacinum,* are among the most potent antiprotozoal agents ever discovered, with some of them being among the most toxic oral mycotoxins known. The term leucinostatin was coined in 1973 for a substance isolated from a fungal fermentation broth. The name leucinostatin was given due to the apparent presence of several leucines, even though the definite structure was yet unsolved.[1] In 1982 Mori et al. demonstrated that the initial leucinostatin[1] was in fact a mixture of several similar compounds and established the structure of the main component leucinostatin A (**1a**) by mass spectrometric, NMR, IR and degradative methods. The compound comprised nine α-amino acid residues, including *cis*-4-methyl-L-proline, (2*S*)-amino-(6*R*)-hydroxy-(4*S*)-methyl-8-oxodecanoic acid (AHMOD), hydroxyleucine and 2-aminoisobutyric amino acids (Aib), as well as fatty acyl moieties consisting of seven carbon atoms at the N-terminus (Figure 1).[2] A year later the same group published the structure of the demethylated derivative leucinostatin B (**1b**).[3] In 1989 the crystal structure of leucinostatin A was established and the α-helical conformation confirmed.[4] With the emergence of tandem mass-spectrometry, more than 20 minor leucinostatin A derivatives with demethylation/oxidation at the N-terminal dimethylamine, the methyl proline, and deletions or changes in the oxidation of the AHMOD sidechain were detected and named alphabetically.[5,6] The total synthesis of leucinostatin A (**1a**) was achieved by Abe et al. (2017), which pointed out the configuration of the previous assumed chirality of the AHMOD side chain hydroxyl group was wrong.[7] The biosynthetic route was studied, and the core biosynthetic genes, which are specific to *P. lilacinum* and *Tolypocladium inflatum ophioglossoides*, were identified.[8]

Since the seminal work by Arai et al., whose new antibiotic leucinostatin consisted of a mixture of leucinostatins A and B,[1] it has become evident that leucinostatins a) inhibit the proliferation of many different organisms and b) are very toxic. The reported effects against pathogens include 21 fungi

[*] Dr. M. Brand, Dr. S. Agnello, Dr. S. Gazzola, F. M. Gall, L. Raguž, Prof. Dr. R. Riedl
Institute of Chemistry and Biotechnology, Center for Organic and Medicinal Chemistry, Zurich University of Applied Sciences (ZHAW)
Einsiedlerstrasse 31, 8820 Wädenswil (Switzerland)
E-mail: rainer.riedl@zhaw.ch
Dr. M. Kaiser, Dr. R. S. Schmidt, A. Ritschl, Prof. Dr. P. Mäser
Swiss Tropical and Public Health Institute
Socinstrasse 57, 4051 Basel (Switzerland),
and
University of Basel
Petersplatz 1, 4001 Basel (Switzerland)
Dr. L. Wang, J. Jelk, Prof. Dr. P. Bütikofer
Institute of Biochemistry and Molecular Medicine, University of Bern
Bühlstrasse 28, 3012 Bern (Switzerland)
Prof. Dr. A. Hemphill
Institute of Parasitology, Vetsuisse Faculty, University of Bern
Länggass-Strasse 122, 3012 Bern (Switzerland)
Dr. M. Adams
Bacoba AG
Elisabethenstrasse 15, 4051 Basel (Switzerland)
E-mail: adams@bacoba.ch
Supporting information and the ORCID identification number(s) for the author(s) of this article can be found under: https://doi.org/10.1002/anie.202102153.

© 2021 The Authors. Angewandte Chemie International Edition published by Wiley-VCH GmbH. This is an open access article under the terms of the Creative Commons Attribution Non-Commercial NoDerivs License, which permits use and distribution in any medium, provided the original work is properly cited, the use is non-commercial and no modifications or adaptations are made.

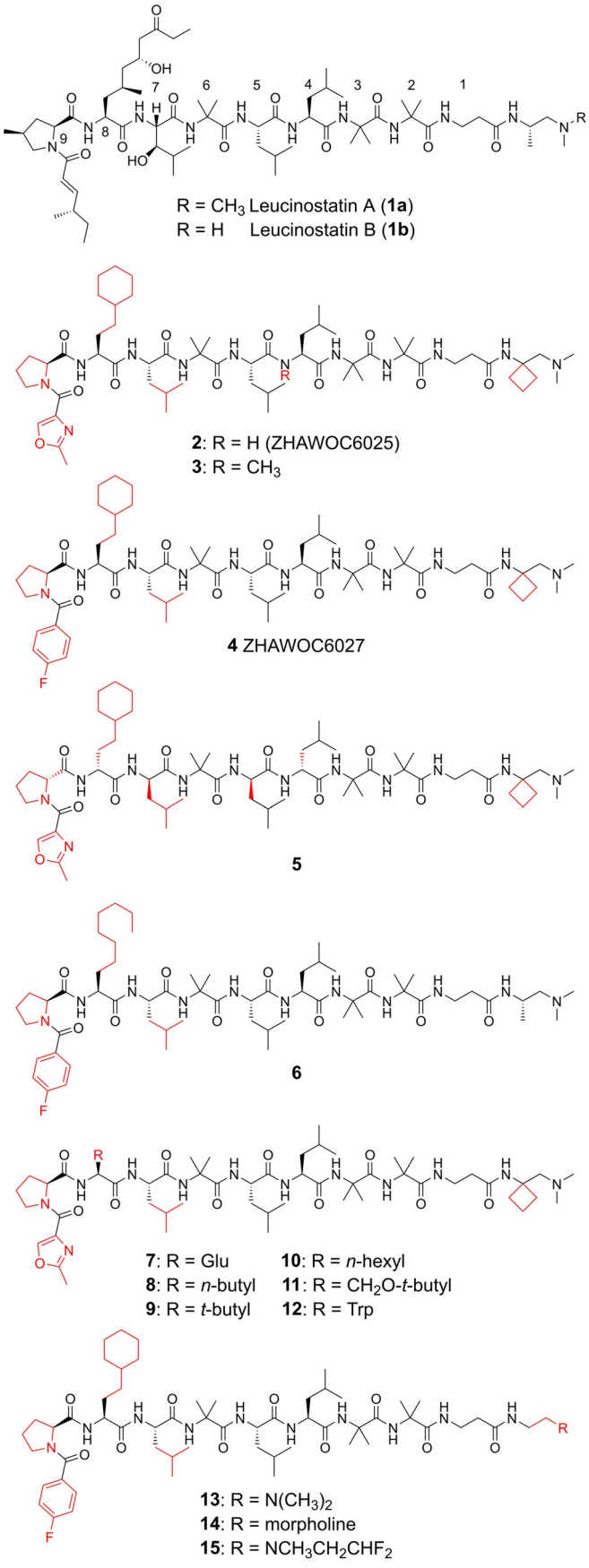

Figure 1. Structural optimization of the natural product leucinostatin A to the simplified derivatives. In red the changes to the natural product are highlighted.

(Minimal Inhibitory Concentrations = MICs: 10–25 μM) and gram-positive bacteria (2.5–100 μM). In addition, leucinostatin was highly toxic in mice with intraperitoneal (ip) LD_{50} of 1.6 mg kg^{-1}. Mikami et al. showed that the ip LD_{50}s of purified leucinostatins A (**1a**) and B (**1b**) were both 1.8 mg kg^{-1}, and the oral LD_{50}s were 5.4 mg kg^{-1} and 6.3 mg kg^{-1}, respectively, and stated that they "belong to a category of the most toxic mycotoxins, such as T-2 toxin, fusarenone-X and aflatoxins".[9] Others have confirmed the acute toxicity, including Ricci et al., whose leucinostatin A (**1a**) had an ip LD_{50} in mice of 1.1 mg kg^{-1}.[10]

This toxicity has prevented the therapeutic use of leucinostatins. Although leucinostatins were first reported as antibiotics,[1] achieving the necessary systemic concentrations (MICs) to eliminate bacterial or fungal pathogens in mammals might exceed their lethal dose.

One group of pathogens, however, the pathogenic protozoa, proved to be hypersusceptible to leucinostatins. Otoguro et al. first showed that leucinostatin A (**1a**) inhibited *Plasmodium falciparum* (the causative agent of malaria tropica) at an IC_{50} of 0.4–0.9 nM, and *Trypanosoma brucei* (the causative agent of Human African Trypanosomiasis (HAT)) at an IC_{50} of 2.8 nM.[11] In the *T. brucei* acute HAT mouse model, leucinostatin B (**1b**) showed curative effects at a dose of 4 × 0.3 mg kg^{-1} ip and 4 × 1.0 mg kg^{-1} ip, whereas leucinostatin A (**1a**) (which was not tested higher due to toxicity) did not at 4 × 0.3 mg kg^{-1} ip.[12] In another HAT acute mouse model, one of 4 mice was cured with leucinostatin B at 4 × 1.0 mg kg^{-1} ip and the mean duration of survival was raised from 11.3 days to 28 days, whilst at 4 × 0.3 mg kg^{-1} ip no mice were cured but the mean duration of survival was slightly increased compared to untreated mice.[12]

The mode of action of leucinostatins has been linked to their general destabilizing effect on biological membranes in both artificial membrane systems and living cells,[13–16] which may explain the non-specific toxicity towards bacteria, fungi, and mammalian cells in the μM range. Leucinostatins are classic peptaibiotics that contain a high proportion of unnatural Aibs, which tend to form 3_{10}-helical structures,[17] and hydrophobic amino acid residues.[18] Leucinostatin belongs to the subclass of AHMOD containing aminolipopeptides.[18]

Little is known about the structural requirement for antiprotozoal activity of leucinostatins and their mode of action. Vertuani et al. obtained eight leucinostatin A homologues by reduction, dehydration and acetylation of the 4-methylhex-2-enoic acid, AHMOD and hydroxy-L-leucine residues, and screened for antibacterial activity.[19] Those subtle modifications did not result in a significant change of the antibacterial activity and had no effect on the secondary structure. Abe et al. performed an alanine scan and reported a concise structure activity relationship (SAR) on tumor cells and tumor-stroma interaction.[20] They reported that the acyl group on the N-terminus is essential for biological activity. Replacement of the unsaturated acyl chain with acetyl resulted in a 1000-fold decrease of the affinity. In addition, alanine scanning revealed that only the replacement of Aib-2 was tolerated, whereas replacement of amino acids Aib-3, Leu-5 and AHMOD-8 reduced the activity by an order of

 © 2021 The Authors. Angewandte Chemie International Edition published by Wiley-VCH GmbH

magnitude. Momose et al. showed that leucinostatin Y, having a carboxylic acid instead of a terminal amine, was far less active against bacteria, fungi, and cancer cells than leucinostatin A (**1a**).[21] However, comprehensive structure–activity relationships (SAR) have not been reported, and pressing issues remain unanswered. Here we present the first comprehensive structure–activity relationship of leucinostatin derivatives, determine the structural imperatives for in vitro antiprotozoal activity, and optimize the selectivity of the molecules.

Results and Discussion

We envisioned to simplify the complex structure of leucinostatin A (**1a**) while maintaining the potency on *T. b. rhodesiense*. The synthetic strategy was based on microwave-assisted solid-phase peptide synthesis (SPPS), followed by a final solution-phase amide coupling of the 9-mer carboxylic acid peptide with the terminal amine (Scheme S1). In the course of the study, the presence of the antiprotozoal pharmacophore was traceable by phenotypic in vitro assays, and we determined which moieties were responsible for the antiprotozoal activity. This led to a comprehensive understanding of the structure–activity relationship.

Replacing the hydroxyleucine at position 7 with a simple and cheap leucine was tolerated and had no negative impact on the biological activity. The Michael acceptor was replaced by either 4-fluorobenzoic acid or an oxazole. The dimethyl amine ethylenamide linker (**6**) on the C-terminus was functionalized with a cyclobutyl amine, as the metabolic stability was thought to be increased and it had little impact on *T. b. rhodesiense* antiprotozoal potency. The side chain does not need to be an AHMOD acid and can be replaced. Ethyl cyclohexyl or *n*-octyl sidechain yielded the most potent compounds, that is, **2**, **4** and **6**, with sub-nanomolar potencies comparable to that of the natural product leucinostatin A (Table 1). These modifications not only maintained the activity against *T. brucei* but also increased the selectivity index between 3- and 5-fold. The hydrophobicity of this side chain is important as modifications, such as replacing it with glutamic acid (**7**) or the shorter *n*-butyl (**8**) aliphatic chain, reduced the in vitro potency, whereas the *n*-hexyl (**10**) analogue still had comparable potency to **2**. It seems that modification of this amino acid has a much bigger influence on parasites compared to the recently published work from Abe et al. on cancer cell lines.[20] The peptide **5**, consisting of unnatural D-amino acids, showed similar activity against *T. b. rhodesiense* as **2** with an IC_{50} of 1.5 nM, meaning both the left and right hand helix are active, which indicates this compound class does not engage with a protein target. Compound **3** *N*-methylated at the leucine amide at position four of the peptide backbone resulted in a 500-fold decrease in activity. Studies on the dimethyl amine at the C-terminus revealed that reducing the basicity of the amine by introduction of a σ-acceptor[22] with either a morpholine (**14**) or a difluoro ethyl methyl amine (**15**) reduced the potency. The experimentally determined pK_a values of the dimethyl amines (**4** and **13**) were 7.3, the morpholine (**14**) had a pK_a of 5.2, and the difluoro ethyl methyl amine (**15**) a $pK_a < 3.5$. As these compounds exhibited the same cytotoxicity (7 μM), it is clear that the increase of basicity changes this compound class from a rather cytotoxic (**15**, selectivity index (SI) 17) to a highly selective compound (**13**, SI 1694).

Table 1: Activity of leucinostatin A and its derivatives on *T. b. rhodesiense* and the cytotoxicity on L6 cells and the calculated selectivity index (SI). The leucinostatin derivatives are compared to the reference drugs melarsoprol, pentamidine and suramin.

compound	*T. b. rhod* [nM]	cytotox L6 [nM]	SI
leucinostatin A (**1a**)	0.25 (0.17–0.36)[a]	259 (97–691)[b]	1036
2	0.76 (0.63–0.91)[d]	3654 (3070–4350)[e]	4808
3	361 (282–461)[a]	> 8449[a]	> 23
4	0.39 (0.35–0.43)[c]	1563 (1322–1848)[c]	4007
5	1.5 (1.1–2.1)[a]	5419 (4804–6113)[a]	3613
6	0.24 (0.20–0.28)[c]	885 (320–2451)[c]	3848
7	> 3200[a]	> 8565[a]	NA
8	6.5 (5.0–8.6)[a]	> 8750[a]	> 1346
9	4.1 (3.1–5.5)[a]	> 8981[a]	> 2190
10	0.85 (0.65–1.1)[b]	5138 (3953–6677)[a]	6045
11	3.9 (2.2–6.8)[a]	> 8749[a]	> 2243
12	1.3 (0.6–3.0)[a]	7101 (5284–9543)[a]	5462
13	3.9 (2.8–5.6)[a]	6608 (4987–8755)[a]	1694
14	72 (52–99)[a]	7169 (5187–9909)[a]	100
15	398 (286–553)[a]	6731 (5597–8095)[a]	17
melarsoprol	5.8 (4.8–7.1)[c]	24220 (15900–36700)[b]	> 4000
pentamidine	1.8 (1.4–2.5)[c]	7600 (5900–9900)[b]	> 4000
suramin	35 (28–44)[c]	> 100000[b]	> 2800

NA = not applicable; [a] $n = 2$; [b] $n = 3$; [c] $n = 4$; [d] $n = 9$, [e] $n = 8$.

 © 2021 The Authors. Angewandte Chemie International Edition published by Wiley-VCH GmbH

Overall, a synthetic, more accessible lead compound was obtained with equipotent activity on *T. b. rhodesiense* but reduced cytotoxicity compared to the natural product. In comparison to the currently available drugs, our synthetic derivatives are superior in regard of their antitrypanosomal potency (Table 1).

In order to gain further insights on the effects of the modifications, analysis of the secondary structure by circular dichroism (CD) spectrometry was performed of leucinostatin A (**1a**), **2**, **3**, **4**, **5**, and **7**. All of the leucinostatin derivatives showed helical character, with the exception of the *N*-methylated compound **3** (supporting information section 3.1), clearly indicating the helix is an important feature for antiprotozoal activity. This shows that methylation of the leucine amide disables helix formation and hence results in massive decrease of anti-parasitic activity.

The helical character of **4** was confirmed by NMR-NOE experiments (Figure S1). Additionally, the kinetics of the deuterium exchange of the backbone amide of **4** in CD_3OD showed that the backbone amide protons 2 to 4 persist with a $t_{1/2} > 1$ hour, with 2 having the longest half-life time of 12.5 hours (Figure S2).

In summary, a helix-forming backbone, the basic terminal amine, and the hydrophobic side chain are crucial for biological activity. As linear peptides are known to be susceptible for fast metabolism, microsomal stability was measured. Both of our lead compounds **2** and **4** showed very encouraging microsomal stability, in particular compound **4** (>80% recovery after 40 minutes, supporting information section 3.5).

Studies on the morphological and cellular effects of the leucinostatin derivatives were done on *T. b. brucei*, which is a subspecies of *T. brucei* and a causative agent of Nagana, a widespread cattle disease in sub-Saharan Africa. It was therefore necessary to establish the inhibitory effects of the experimental compounds on *T. b. brucei* as well. The activities of leucinostatin A (**1a**) (0.4 nM), **2** (6.4 nM), **4** (3.6 nM) and **7** (>1000 nM) were comparable to the values obtained against *T. b. rhodesiense*.

Confirmation of In Vivo Efficacy

Compounds **2** (ip 3 mg kg^{-1} twice a day (bid) for 4 days, and orally (po) 30 mg kg^{-1} once a day (qd) for 4 days) and **4** (ip 3 mg kg^{-1} bid 2 days) were tested for in vivo efficacy using the *T. b. brucei* (STIB795) acute NMRI mouse model. The mice had no detectable parasitemia (<10^4 parasites mL^{-1}) after the treatment with **2** (for 4 days) and **4** (for 2 days). The survival of mice was prolonged compared to the untreated controls (Figure 2). Interestingly, **2** (po 30 mg kg^{-1} qd 4 days) was active also when given orally.

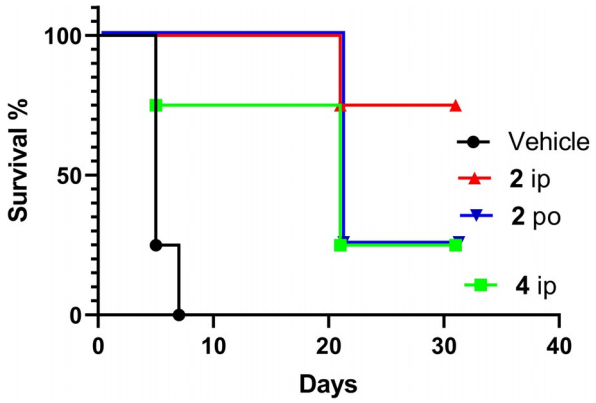

Figure 2. Kaplan-Meier plot of the in vivo experiment on *T. b. brucei* (STIB795) acute NMRI mouse model treated with vehicle, **2** (ip and po) and **4** (ip). $n = 4$.

Mode of Action

Earlier studies have shown that leucinostatin A (**1a**) can act as a ionophore on isolated mitochondrial and chloroplast preparations[13–15] and increase membrane permeability of cells and artificial membranes by facilitating transport of monovalent and divalent cations.[14] In addition, in model liposomes, leucinostatin A underwent concentration-dependent self-aggregation in the lipid bilayer, thereby affecting lipid phase transition and membrane fluidity, and causing membrane pore formation.[15] Similar observations have been made for other cationic antimicrobial peptides, such as melittin and magainin, which cause membrane damage by inserting into lipid bilayers and forming transient or stable pores.[23,24] Such pores may allow membrane lipids to freely diffuse from one side of the bilayer to the other and small hydrophilic molecules to cross the membrane. To study if the leucinostatin derivatives synthesized in the present study are capable of inducing transbilayer scrambling of phospholipids, peptides were added to liposomes composed of egg phosphatidylcholine (PC), egg phosphatidylglycerol (PG) and trace amounts of [^{3}H]-labelled phosphatidylinositol ([^{3}H]PI), with the label at the inositol, and treated with PI-specific phospholipase C (PI-PLC). In control liposomes, treatment by PI-PLC should result in hydrolysis of approximately 50% of [^{3}H]PI, that is, the portion of [^{3}H]PI present in the outer leaflet of the bilayer (Figure 3a). In contrast, if leucinostatins induce transbilayer movement of phospholipids, all [^{3}H]PI should be available to PI-PLC after addition of peptides to liposomes (Figure 3a).[25] The extent of [^{3}H]PI hydrolysis increased from 50% in control liposomes to >80% in liposomes after addition of increasing amounts of peptides **1a**, **2** or **4** (Figure 3b). These results are consistent with peptide-induced translocation of [^{3}H]PI from the inner to the outer leaflet of liposomes. In contrast, no redistribution of [^{3}H]PI was observed after addition of the non-antiprotozoal peptide **7** to liposomes (Figure 3b).

In addition, the formation of membrane pores was assayed using liposomes containing trapped NBD-glucose. In control liposomes, NBD-glucose remains in the lumen of the liposomes and, thus, its fluorescence cannot be reduced by membrane-impermeable dithionite present in the solution (Figure 3c). In contrast, if the addition of peptides to liposomes results in pore formation, entrapped NBD-glucose can diffuse out of the liposomes, or alternatively dithionite can enter the liposomes, and NBD fluorescence will be

 © 2021 The Authors. Angewandte Chemie International Edition published by Wiley-VCH GmbH

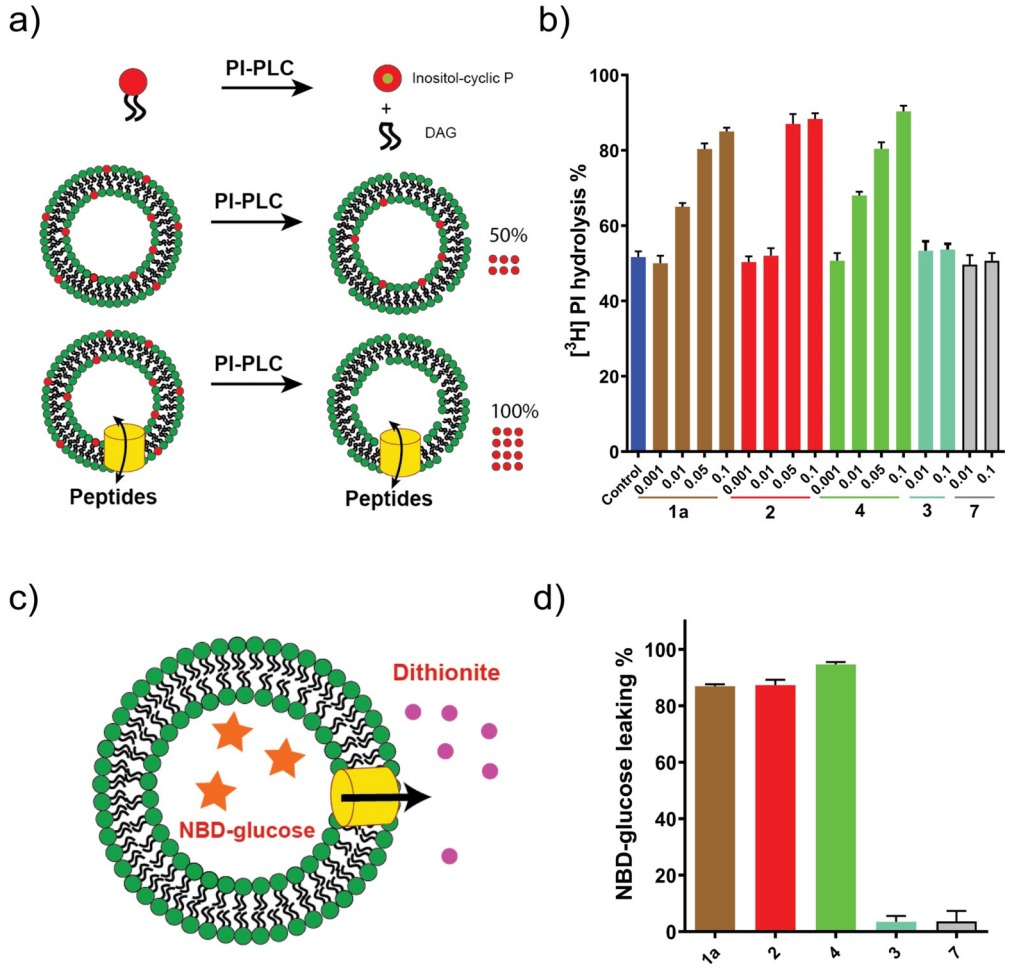

Figure 3. a) Schematic representation of PI-PLC assay. Incubation of unilamellar liposomes composed of egg PC and egg PA (3:1, molar ratio; green symbols) and trace amounts of [^{3}H]PI (red symbols) with PI-PLC results in hydrolysis of [^{3}H]PI (to inositol cyclic phosphate and diacylglycerol (DAG)) in the outer leaflet of the bilayer while [^{3}H]PI in the inner leaflet is protected from the enzyme. As [^{3}H]PI distributes equally between the two leaflets during preparation of liposomes, approximately 50% is expected to be hydrolyzed by PI-PLC. In unilamellar liposomes reconstituted with peptides, [^{3}H]PI from the inner leaflet is translocated to the outer leaflet, where it becomes accessible to PI-PLC. b) Scrambling activity of peptides **1a**, **2**, **3**, **4** and **7** are shown in a dose response with a peptide phospholipid ratio between 0.001 to 0.1. c) Schematic representation of the trapped NBD-glucose assay. Unilamellar liposomes trapped with NBD-glucose (orange star) are treated with peptides. If a leakage occurs upon peptide addition, the NBD labelled glucose will be quenched by dithionite (purple symbol) and the decrease of the fluorescence signal is measured. d) NBD-glucose leakage by the addition of peptide **1a**, **2**, **3**, **4** and **7** at a phospholipid peptide ratio (PPR) of 0.1.

reduced (Figure 3c). Addition of compounds **1a**, **2** and **4** to NBD-glucose loaded liposomes led to complete loss of fluorescence (Figure 3d). In contrast, no reduction was observed after addition of peptide **7**, indicating that peptides **1a**, **2** and **4** induced pore formation in liposomes while peptide **7** was inactive. The above findings, that is, complete hydrolysis of [^{3}H]PI by PI-PLC and reduction of NBD-glucose by dithionite, could also result from peptide-induced lysis of liposomes. However, examination by electron microscopy revealed that liposomes after peptide treatment were indistinguishable from control liposomes (Figure S3), ruling out that the peptides acted as detergents causing lysis of the liposomes.

To analyse leucinostatin activity on live trypanosomes, *T. b. brucei* bloodstream forms were treated with compound **2** for 24 h before parasites were incubated with the mitochondrial membrane potential-dependent dye MitoTracker and examined by fluorescence microscopy. The typical mitochondrial staining of control trypanosomes was completely absent in parasites treated with compound **2** (Figure 4a,b), indicating that addition of compound **2** resulted in loss of mitochondrial membrane potential. Similar results were obtained with compounds **4** and **5** (40 nM, final concentration). In contrast, no changes in MitoTracker staining was observed when *T. brucei* bloodstream forms were treated with compounds **3** and **7**. To corroborate these findings, we quantified the mitochondrial membrane potential in parasites before and after drug treatment using the mitochondrial membrane-potential dye TMRE. Treatment of trypanosomes with compounds **1a**, **2**, **4** and **5** resulted in a concentration-dependent decrease of TMRE fluorescence relative to control parasites (Figure 4c), reflecting drug-induced loss of mitochondrial membrane potential. In contrast, no changes in fluorescence were observed for compounds **3** and **7** (Figure 4c).

 © 2021 The Authors. Angewandte Chemie International Edition published by Wiley-VCH GmbH

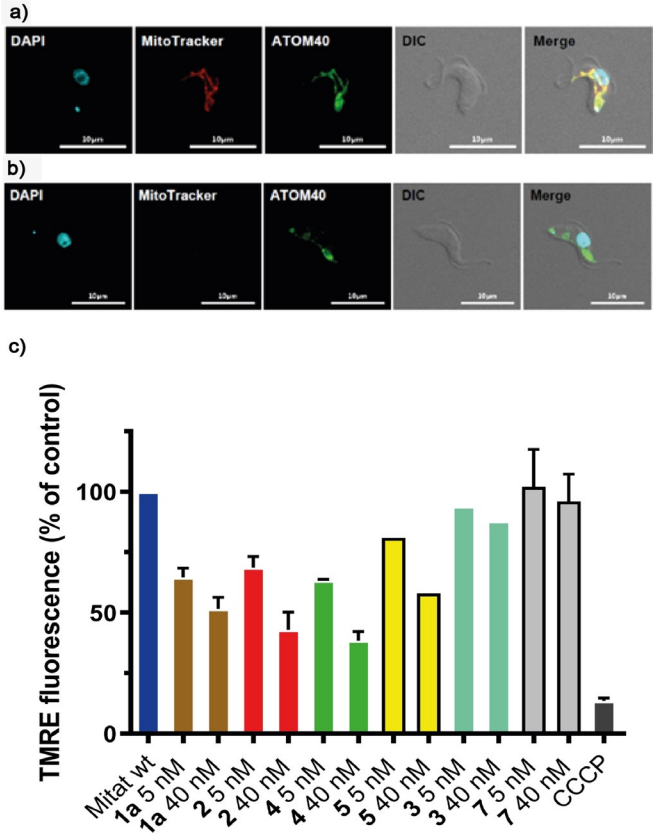

Figure 4. Qualitative and quantitative immunofluorescence staining of NYsm parasites. a) Untreated NYsm parasites were stained with 4′,6-diamidino-2-phenylindole (DAPI), MitoTracker and anti-ATOM40. b) NYsm parasites were treated with **2** for one day and stained with DAPI, MitoTracker and anti-ATOM40. c) The quantitative measurement of the mitochondrial membrane potential with compounds **1a**, **2**, **3**, **4**, **5** and **7**. The positive control carbonyl cyanide m-chlorophenyl hydrazone (CCCP) is also shown. DIC = differential interference contrast.

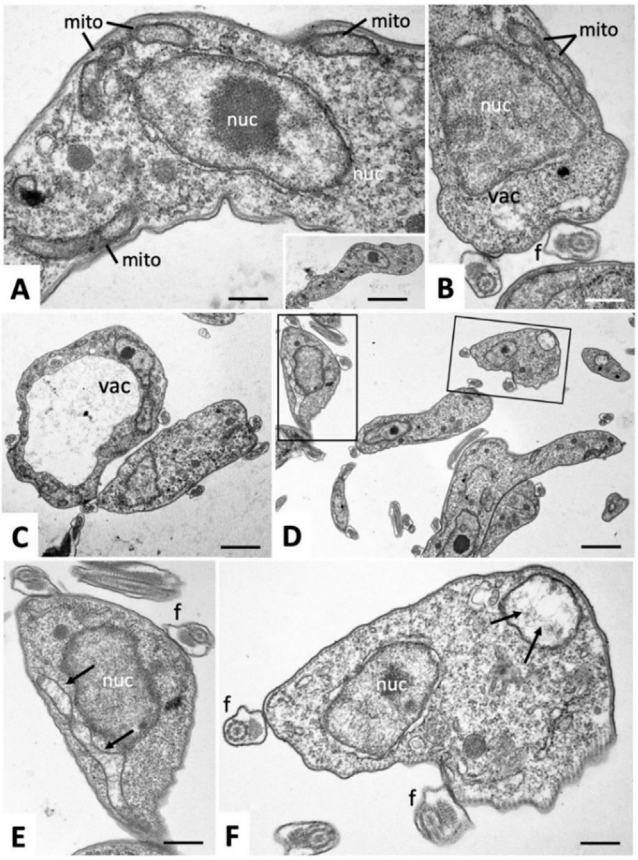

Figure 5. TEM Transmission electron micrographs of *T. b. brucei* bloodstream forms. A shows a higher magnification view of the cytoplasm of a non-treated control, the insert is the corresponding lower magnification view. Nucleus (nuc) and parts of the mitochondrion with an electron dense matrix are discernible. Bar in A = 0.25 μm; insert = 1.2 μm. B and C represent parasites treated with 5 nM **4** for 2 h. The mitochondrion (mito) retained an electron dense matrix, but in many cases, parasites exhibited different degrees of vacuolization (vac). Bar in B = 0.35 μm, C = 0.8 μm. In D, E and F parasites were treated with 40 nM **4** for 2 h. D is a low magnification overview, the boxed areas are magnified in E and F. The visible parts of the mitochondrion have lost their characteristic electron dense matrix (black arrows in E, F), and appear rounded and enlarged (F). The ultrastructure of the flagellum (f) remains unaltered. Bars in D = 1.2 μm; *E* = 0.45 μm; F = 0.3 μm.

Furthermore, examination of drug-treated trypanosomes by transmission electron microscopy revealed changes in mitochondrial ultrastructure, with the mitochondrial matrix appearing less electron dense, while other intracellular structures seemed unaffected (Figure 5). No changes were seen when drug-treated parasites were examined by scanning electron microscopy (Figure S4). Together, these results demonstrate that compounds **1a**, **2**, **4**, and **5** act on *T. b. brucei* bloodstream forms by affecting mitochondrial ultrastructure and causing loss of mitochondrial membrane potential.

In Vitro Selection for Drug Resistance

To learn more about the mechanisms of trypanocidal drug action, we attempted to select for drug-resistant mutants. Bloodstream-form *T. b. brucei* of the "New York single-marker" strain (NYsm)[26] were exposed to sublethal concentrations (0.5 nM–1.5 nM) of **2** in vitro. The cultures were maintained and eventually sub-passaged in drug-containing medium. However, there was no indication of developing drug resistance. Parasite cultures always died off within a couple of days when exposed to 1.5 nM **2**, even after 7 months of selection. This may indicate that **2** disrupts a fundamental process, which cannot readily be overcome by a mutation in a single gene.

Having failed to obtain drug-resistant trypanosomes by forward selection, we applied a reverse genetic approach to select for resistance. For this purpose, an RNAi library transfected into *T. b. brucei* NYsm was used,[27] which consisted of about 12′000 pooled transfectants, each expressing a different small interfering RNA (siRNA) under the control of a tetracycline promoter. This approach is powerful for selecting loss-of-function mutants that exhibit drug resistance when the expression of a particular gene is down-regulated.[27] However, no resistant cells were obtained upon induction of siRNA expression by addition of 1 $\mu g\,mL^{-1}$

 © 2021 The Authors. Angewandte Chemie International Edition published by Wiley-VCH GmbH

tetracycline followed by selection with **2** at 8.6, 17.1, or 25.7 nM. Eflornithine was used as a positive control for drug selection and resulted in the identification of the amino acid transporter TbAAT6, as demonstrated before.[27]

In Vitro Pharmacodynamic Parameters

Isothermal microcalorimetry[28,29] was performed with the two lead compounds **2** and **4** to monitor their trypanocidal action in real time (Figure S5). The two compounds were studied at one- to thirty-fold their EC_{50} (1 to 30 nM for **2**; 0.5 to 15 nM for **4**).

Dose-dependent growth inhibition was observed for both molecules, that is, for **2** at 3 nM and for **4** at 1.5 nM, and substantially reduced growth of bloodstream-form *T. b. rhodesiense*, but failed to kill all parasites.

At 5 nM **4** or 10 nM **2**, the parasites were quickly killed within 24 hours (Table 2). Time to kill was also dose-dependent. Onset of drug action was very fast for both leucinostatin derivatives (Table 2).

Table 2: Isothermal calorimetry measurements with a dose response measurement of **2** and **4**. With an increasing inhibitor concentration, the time to peak and time to kill were shortened.

compound	conc. [nM]	drug action onset [h]	time to peak [h]	time to kill [h]
drug free			38.3 ± 0.8	108 ± 1
2	1.0	2.2 ± 0.7	39.9 ± 0.8	115 ± 5
	3.0	3.3 ± 2.6	35.3 ± 4.2	101 ± 15
	10	< 2	12.8 ± 1.1	27 ± 2.6
	30	< 2	15.2 ± 1.5	31 ± 3.3
4	0.5	5.5 ± 6	40.0 ± 2.5	112 ± 6
	1.5	4.2 ± 2.1	33.5 ± 3.2	97 ± 13
	5.0	< 2	10.8 ± 1.3	23 ± 0.9
	15	< 2	13.7 ± 2.3	28 ± 3.5

Activity on further Protozoan Parasites

Encouraged by the high degree of activity of leucinostatin A and its derivatives against *T. brucei*, we tested the lead compounds **2** and **4** and tool compounds **3**, **5** and **7** also against the protozoan parasites *Trypanosoma cruzi* (causative agent of Chagas disease), *Leishmania donovani* (visceral leishmaniasis), *Plasmodium falciparum* (malaria tropica) (Table 3).

Table 3: Activities of leucinostatin A (**1a**), **2**–**5** and **7** on different parasitic strains including the positive control compounds (miltefosin, benznidazole and chloroquine).

compound	*L. donovani.* axenic amastigotes [nM]	*L. donovani.* Macrophage [nM]	*T. cruzi* [nM]	*P. falciparum* NF54 [nM]
1a	1.05[b] (0.96–1.15)	9.8[a] (5.0–19)	23[c] (16–33)	0.61[c] (0.27–1.40)
2	11[c] (9.1–14)	18[c] (7.4–42)	193[f] (145–258)	4.8[e] (3.9–5.7)
3	9259[b] (6201–13820)	ND	> 2000[b]	591[b] (535–654)
4	4.9[c] (3.1–7.9)	50 (39–64)[b]	114[d] (92–142)	5.4[d] (4.3–6.6)
5	4.8[b] (3.3–7.1)	ND	311 (190–510)[b]	26[b] (22–30)
7	> 8565[b]	ND	> 2000[b]	> 8565[b]
miltefosine	483[d] (402–580)	4912[d] (3415–7065)	ND	ND
benznidazol	ND	ND	1925[d] (1522–2435)	ND
chloroquine	ND	ND	ND	4.9[d] (3.8–6.2)

ND = not determined; [a] $n = 1$; [b] $n = 2$; [c] $n = 3$; [d] $n = 4$; [e] $n = 6$; [f] $n = 8$.

The IC_{50} values were in the nM range, except for **3** and **7** (Table 3), closely matching the results obtained in the *T. brucei* assay.

Low nM IC_{50} values were seen against the axenically grown amastigotes of *L. donovani.* The IC_{50} values of **2** and **4** on intracellular *L. donovani* were 18 nM and 50 nM, respectively, indicating that the compounds have excellent cell penetrating properties. This was confirmed in intracellular *T. cruzi* parasites. Intra-erythrocytic *P. falciparum* were also inhibited by **2** and **4** at 4.8 nM and 5.4 nM, respectively.

Conclusion

Developing peptides as drug candidates poses several extra challenges as compared to small molecules, which has limited their widespread use. One aspect is the inherent biological instability of xenobiotic peptides and their rapid enzymatic degradation in the body, limiting exposure. Nevertheless, peptide therapeutics continue to be in the focus of current drug discovery and development projects due to their distinct biological activities in academia as well as industry and show increasing success rates.[30]

Previous reports showed that leucinostatin A was toxic by both oral and ip administration.[12,31] Synthetic modifications of the natural product leucinostatin A by removal of the Michael acceptor and replacement of the AHMOD amino acid with either *n*-octyl or ethyl cyclohexyl moiety resulted in equipotent derivatives. Compounds **2** and **4** inhibited growth

 © 2021 The Authors. Angewandte Chemie International Edition published by Wiley-VCH GmbH

of protozoan parasites in the low nanomolar range, and disrupted artificial liposomes in the same concentration range, without dissolving, disintegrating or lysing them. The active compounds allowed phospholipids to scramble from one half of the bilayer to the other. Interestingly, *T. brucei* parasites remained structurally intact, but lost the functionality of certain membrane systems, most notably the inner mitochondrial membrane.

The leucinostatin derivatives exhibited the same SAR against trypanosomes and liposomes. We determined the α-helical nature of the compound, the protonation of the terminal amine, and the hydrophobicity of the side chain to be essential in both test systems, indicating the same mode of action in each. The fast onset of the drug action as measured by isothermal microcalorimetry supports this conclusion.

Destabilization of the inner mitochondrial membrane represents a mode of action that incapacitates cells at a very fundamental level and to which they cannot readily develop resistance. This was shown by exposing *T. brucei* parasites to sublethal doses of **2** for seven months, as well as by screening against 12′000 siRNA knock-down mutants—none of which developed resistance.

In comparison to the clinical approved drugs melarsoprol, pentamidine and suramin, compounds **2** (ZHAWOC6025) and **4** (ZHAWOC6027) are superior in their ability to kill *T. brucei* parasites and, perhaps more importantly, showed no signs of developing drug resistance. The inhibitors **2** and **4** represent a novel compound class for the treatment of *T. brucei* infections and should be considered for application against other parasitic diseases as well.

Acknowledgements

We acknowledge the generous and continuous financial support by the Swiss Agency for Technology and Innovation (CTI) and Innosuisse (research grants 16445.1 PFLS-LS, 19208.1 PFPL-LS and 34227.1 IP-LS to R. Riedl and the ZHAW medicinal chemistry team). A. Hemphill was supported by Swiss National Science Foundation (SNSF) grant 310030_184662 and P. Bütikofer by SNSF grant 31003A_169355. L. Wang received financial support from grant no. 881 by The Velux Foundation (to P. Bütikofer and Anant K. Menon). We kindly acknowledge Isabel Roditi (Institute of Cell Biology, University of Bern) for providing the RNAi library. We thank M. Cal, R. Rocchetti and S. Keller-Märki for help with antiparasitic drug testing. We also acknowledge Aitor Moreno and Sandra Loss (Bruker Switzerland AG, Fällanden) for NOE measurements on the 800 MHz NMR instrument.

Conflict of interest

M. Adams is currently CEO of Bacoba AG, who supported this research scientifically, financially, and logistically. The use of those compounds is protected by patent EP3345917.

Keywords: antiparasitic agent · drug discovery · medicinal chemistry · mode of action · peptides

[1] T. Arai, Y. Mikami, K. Fukushima, T. Utsumi, K. Yazawa, *J. Antibiot.* **1973**, *26*, 157 – 161.
[2] Y. Mori, M. Tsuboi, M. Suzuki, K. Fukushima, T. Arai, *J. Chem. Soc. Chem. Commun.* **1982**, 94 – 96.
[3] Y. Mori, M. Suzuki, K. Fukushima, T. Arai, *J. Antibiot.* **1983**, *36*, 1084 – 1086.
[4] S. Cerrini, D. Lamba, A. Scatturin, G. Ughetto, *Biopolymers* **1989**, *28*, 409 – 420.
[5] A. Isogai, J. Nakayama, S. Takayama, A. Kusai, A. Suzuki, *Biosci. Biotechnol. Biochem.* **1992**, *56*, 1079 – 1085.
[6] A. F. C. Martinez, L. A. B. Moraes, *J. Antibiot.* **2015**, *68*, 178 – 184.
[7] H. Abe, H. Ouchi, C. Sakashita, M. Kawada, T. Watanabe, M. Shibasaki, *Chem. Eur. J.* **2017**, *23*, 11792 – 11796.
[8] G. Wang, Z. Liu, R. Lin, E. Li, Z. Mao, J. Ling, Y. Yang, W.-B. Yin, B. Xie, *PLOS Pathog.* **2016**, *12*, e1005685.
[9] Y. Mikami, K. Fukushima, T. Arai, F. Abe, H. Shibuya, Y. Ommura, *Zentralbl. Bakteriol. Mikrobiol. Hyg. Abt. 1 Orig. A* **1984**, *257*, 275 – 283.
[10] M. Ricci, P. Sassi, C. Nastruzzi, C. Róssi, *AAPS PharmSciTech* **2000**, *1*, 9 – 19.
[11] K. Otoguro, H. Ui, A. Ishiyama, N. Arai, M. Kobayashi, Y. Takahashi, R. Masuma, K. Shiomi, H. Yamada, S. Omura, *J. Antibiot.* **2003**, *56*, 322 – 324.
[12] A. Ishiyama, K. Otoguro, M. Iwatsuki, M. Iwatsuki, M. Namatame, A. Nishihara, K. Nonaka, Y. Kinoshita, Y. Takahashi, R. Masuma, K. Shiomi, H. Yamada, S. Omura, *J. Antibiot.* **2009**, *62*, 303 – 308.
[13] K. Ishiguro, T. Arai, *Antimicrob. Agents Chemother.* **1976**, *9*, 893 – 898.
[14] P. Csermely, L. Radics, C. Rossi, M. Szamel, M. Ricci, K. Mihály, J. Somogyi, *Biochim. Biophys. Acta Mol. Cell Res.* **1994**, *1221*, 125 – 132.
[15] M. Fresta, M. Ricci, C. Rossi, P. M. Furneri, G. Puglisi, *J. Colloid Interface Sci.* **2000**, *226*, 222 – 230.
[16] K. R. Sridhar, *Frontiers in Fungal Ecology, Diversity and Metabolites*, I.K. International Pvt Ltd, Dehli, **2008**.
[17] G. R. Marshall, E. E. Hodgkin, D. A. Langs, G. D. Smith, J. Zabrocki, M. T. Leplawy, *Proc. Natl. Acad. Sci. USA* **1990**, *87*, 487 – 491.
[18] L. A. Stubbing, I. Kavianinia, M. A. Brimble, *Org. Biomol. Chem.* **2017**, *15*, 3542 – 3549.
[19] G. Vertuani, M. Boggian, A. Scatturin, M. Ricci, B. Meli Balbocchino, L. Tuttobello, C. Rossi, *J. Antibiot.* **1995**, *48*, 254 – 260.
[20] H. Abe, M. Kawada, C. Sakashita, T. Watanabe, M. Shibasaki, *Tetrahedron* **2018**, *74*, 5129 – 5137.
[21] I. Momose, T. Onodera, H. Doi, H. Adachi, M. Iijima, Y. Yamazaki, R. Sawa, Y. Kubota, M. Igarashi, M. Kawada, *J. Nat. Prod.* **2019**, *82*, 1120 – 1127.
[22] M. Morgenthaler, E. Schweizer, A. Hoffmann-Röder, F. Benini, R. E. Martin, G. Jaeschke, B. Wagner, H. Fischer, S. Bendels, D. Zimmerli, J. Schneider, F. Diederich, M. Kansy, K. Müller, *ChemMedChem* **2007**, *2*, 1100 – 1115.
[23] A. Marquette, B. Bechinger, *Biomolecules* **2018**, *8*, 18.
[24] M. Hasan, M. M. R. Moghal, S. K. Saha, M. Yamazaki, *Biophys. Rev.* **2019**, *11*, 431 – 448.
[25] L. Wang, Y. Iwasaki, K. K. Andra, K. Pandey, A. K. Menon, P. Bütikofer, *J. Biol. Chem.* **2018**, *293*, 18318 – 18327.
[26] E. Wirtz, S. Leal, C. Ochatt, G. A. Cross, *Mol. Biochem. Parasitol.* **1999**, *99*, 89 – 101.
[27] G. Schumann Burkard, P. Jutzi, I. Roditi, *Mol. Biochem. Parasitol.* **2011**, *175*, 91 – 94.

 © 2021 The Authors. Angewandte Chemie International Edition published by Wiley-VCH GmbH

[28] T. Wenzler, A. Steinhuber, S. Wittlin, C. Scheurer, R. Brun, A. Trampuz, *PLoS Neglected Trop. Dis.* **2012**, *6*, e1668.
[29] M. Gysin, O. Braissant, K. Gillingwater, R. Brun, P. Mäser, T. Wenzler, *Int. J. Parasitol. Drugs Drug Resist.* **2018**, *8*, 159 – 164.
[30] A. T. Zizzari, D. Pliatsika, F. M. Gall, T. Fischer, R. Riedl, *Drug Discov. Today* **2021**, https://doi.org/10.1016/j.drudis.2021.01.020.
[31] Y. Mikami, K. Fukushima, T. Arai, F. Abe, H. Shibuya, Y. Ommura, *Zentralbl. Bakteriol. Mikrobiol. Hyg. Ser. A* **1984**, *257*, 275 – 283.

Manuscript received: February 10, 2021
Revised manuscript received: March 13, 2021
Accepted manuscript online: March 17, 2021
Version of record online: May 10, 2021

 © 2021 The Authors. Angewandte Chemie International Edition published by Wiley-VCH GmbH